Effect of frequency chirp on soliton spectral sidebands in fiber lasers

L. W. Liou and Govind P. Agrawal

The Institute of Optics, University of Rochester, Rochester, New York 14627

Received February 24, 1995

Fiber lasers emit soliton pulses that exhibit discrete spectral sidebands generated through dispersive-wave resonances. The position of these soliton sidebands is shown to be affected by the amount of chirp acquired by the pulse, and the degree of chirp is determined by total cavity losses and gain dispersion. Our results show that the soliton chirp shifts the sideband frequencies and that sidebands can be generated even in the case of normal dispersion. The long- and short-cavity cases are discussed separately so that our results are applicable to all laser configurations.

The spectrum of soliton pulses emitted by mode-locked fiber lasers exhibits sidebands whose origin is well understood.[1–6] The sidebands result from a constructive interference between the soliton and dispersive waves and occur at frequencies for which their relative phase difference is a multiple of 2π. In previous studies[1–6] the sideband frequencies were determined under the assumption of a chirp-free soliton, similar to that formed in passive (undoped) fibers. In the case of active fibers the gain dispersion imposes a frequency chirp such that the mode-locked pulses emitted by a fiber laser correspond to chirped solitons.[7,8] This Letter shows that such a frequency chirp modifies the interference condition and shifts the frequencies of the side modes generated through the dispersive-wave resonances.

The evolution of mode-locked pulses in fiber lasers is governed by a master equation that incorporates the effects of fiber dispersion and nonlinearity, gain and gain dispersion, and effective saturable absorption leading to passive mode locking.[7] This equation is a generalized nonlinear Schrödinger equation (or a Ginzburg–Landau equation) and in its normalized form can be written as[8]

$$\frac{\partial A}{\partial \xi} + \frac{i}{2}(s + id)\frac{\partial^2 A}{\partial \tau^2} - i(1 - i\delta)|A|^2 A = \frac{1}{2}\mu A, \quad (1)$$

where A is the normalized slowly varying amplitude, $\xi = z/L_D$, $\tau = t/T_c$, and the parameters s, d, and μ are defined as

$$s = \mathrm{sgn}(\beta_2), \qquad d = g_0 L_D, \qquad \mu = (g_0 - \alpha_0)L_D, \quad (2)$$

and $\delta = \alpha_0\lambda/4\pi n_2 I_s$ is a measure of the saturable absorption in the system, which is of the order of 0.1 for a passively mode-locked erbium-doped fiber laser. Here n_2 is the nonlinear index coefficient, $L_D = T_c^2/|\beta_2|$ is the dispersion length, β_2 is the dispersion parameter, g_0 is the small-signal gain coefficient, and we include saturable absorption by writing the net peak gain as $g_p = g_0 - \alpha_0(1 - I/I_s)$, where α_0 is the small-signal absorption coefficient, I is the pulse intensity, and I_s is the saturation intensity. If the laser cavity contains both doped and undoped fibers, the parameters β_2, g_0, and α_0 are averaged over the cavity length. Typically $\alpha_0 \ll g_0$, so the normalized gain of the laser is simply taken to be $\mu = g_0 L_D$. In deriving Eq. (1) the gain spectrum is approximated by a parabola as $g(\omega) = g_0[1 - T_c^2(\omega - \omega_0)^2]$. We obtain reasonable results by setting $T_c = 1$ ps. The parameter T_c is related to the curvature of the gain spectrum at the lasing wavelength and is typically ~1 ps. Note that Eq. (1) is general enough to describe any fiber laser configuration (linear, ring, or figure-eight), as long as the parameter δ is determined appropriately for the process of additive-pulse mode locking.[7]

The solitary-wave solution of Eq. (1) is well known and is given by[7–10]

$$A(\xi, \tau) = N[\mathrm{sech}(p\tau)]^{(1+iq)}\exp(i\Gamma\xi), \quad (3)$$

where the soliton amplitude N, the width parameter p, and the propagation constant Γ are determined from

$$N^2 = \frac{p^2}{2}[s(q^2 - 2) + 3qd], \quad (4)$$

$$p^2 = -\mu[d(1 - q^2) + 2sq]^{-1}, \quad (5)$$

$$\Gamma = \frac{p^2}{2}[2qd - s(1 - q^2)] \quad (6)$$

and q is the chirp parameter, whose value is determined by the quadratic equation

$$(d + s\delta)q^2 - 3(s - d\delta)q - 2(d + s\delta) = 0. \quad (7)$$

Clearly, if $q \neq 0$, the soliton described by Eq. (3) is chirped. Since q is generally not zero, the pulses formed inside a fiber laser are chirped solitons. As seen in Eq. (7), the amount of chirp on the pulse is determined by the gain dispersion d, the saturable absorption parameter δ, and the sign of the dispersion parameter.

Figure 1 shows the chirp parameter q and the full width at half-maximum (FWHM), $T_{\mathrm{FWHM}} = 1.76T_c/p$, of the chirped solitons as a function of the amplifier gain (in decibels) $G = \exp(g_0 L)$ for the anomalous dispersion (solid curves) and normal dispersion (dashed curves)

0146-9592/95/111286-03$6.00/0

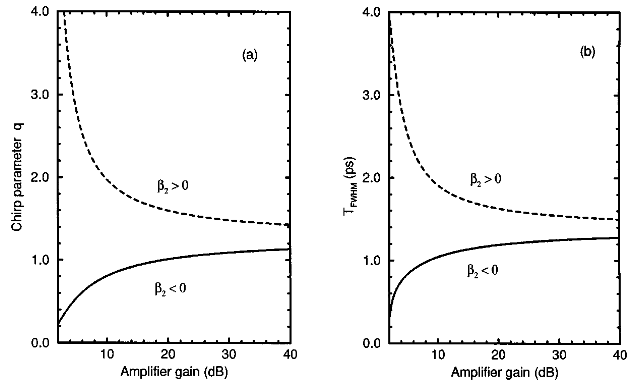

Fig. 1. (a) Chirp parameter q and (b) the FWHM of the chirped soliton pulse as a function of the amplifier gain for the anomalous (solid curves) and normal (dashed curves) dispersion regimes.

regions by the choice of $T_c = 1$ ps and $\delta = 0.1$. The chirp is given by $-d\phi/d\tau$, where ϕ is the phase of the soliton and is of the form $qp\tanh(p\tau)$. From Fig. 1(a) we note that the soliton acquires a positive chirp for both normal and anomalous dispersion. For relatively small values of gain there are no real values of chirp and pulse width that permit the chirped soliton to be a solution to Eq. (1). In this limit in which the gain approaches zero the model that includes saturation absorption becomes invalid. In practice, the saturated gain must equal the cavity loss, and the amplifier gain G is expected to be fairly large (>10 dB) for compensation of cavity losses. Interestingly, the amount of chirp acquired by a soliton in the laser cavity is dependent on the amount of round-trip cavity losses. Figure 1(b) shows that the mode-locked pulses are broader in the case of normal dispersion ($\beta_2 > 0$), but the difference becomes small for large gain since gain dispersion dominates the index-dispersion effects of the host fiber. The predicted pulse width of ~1 ps depends on the choice of T_c, which can be used as a fitting parameter. For relatively small values of gain the chirp and the pulse width in the normal dispersion regime become quite large. This is not surprising since solitons are not supported in this regime in undoped fibers.

What are the consequences of the frequency chirp that is invariably imposed on the pulses circulating inside a fiber laser? It turns out that the spectral sidebands generated through dispersive-wave resonances are shifted from the frequencies expected in the absence of frequency chirp. We can easily understand the reason by noting that the soliton propagation constant Γ in Eq. (3) depends on the chirp parameter q. Since the interference condition depends on the soliton phase shift acquired during one round trip (and the phase shift depends on Γ), the sideband frequencies also become a function of the chirp parameter q. Mathematically the relative phase difference $|\beta_s(\omega_0) - \beta(\omega_0 + \delta\omega)|L$ between the soliton at the frequency ω_0 and the dispersive wave at the frequency $\omega_0 + \delta\omega$ must be an integer multiple of 2π for constructive interference to occur,[5] where $\beta_s(\omega_0) = \beta(\omega_0) + \Gamma/L_D$ is the soliton wave number at the carrier frequency ω_0. By expanding $\beta(\omega + \delta\omega)$ in a Taylor series and retaining up to the quadratic term (the linear term corresponds to a change in the group velocity) we obtain the angular frequency of the mth sideband:

$$\delta\omega^2 = \frac{p^2}{|\beta_2|L_D}\left[\frac{-4\pi smL_D}{p^2L} - (1 - q^2 - 2sqd)\right], \qquad (8)$$

where $s = +1$ or -1, depending on the sign of β_2, and m is an integer. It is useful to introduce the soliton width as $T_s = T_c/p$ and define the soliton period as $z_0 = \pi T_s{}^2/(2|\beta_2|)$. Using $L_D = T_c{}^2/|\beta_2|$ in Eq. (8) and introducing $\delta\nu_m = \delta\omega_m/2\pi$ as the frequency of the mth sideband, we obtain

$$\delta\nu_m = \pm\frac{0.28}{T_{\mathrm{FWHM}}}\left[\frac{-s8mz_0}{L} - (1 - q^2 - 2sqd)\right]^{1/2}, \qquad (9)$$

where $T_{\mathrm{FWHM}} = 1.76T_s$ is the FWHM of the soliton.

Equation (9) is the main result of this study. It reduces to the previously obtained result[1–5] if we neglect the soliton chirp by setting $q = 0$ and assume the dispersion to be anomalous ($s = -1$). Our Eq. (9) not only predicts that the soliton chirp shifts the sideband frequencies but also shows that sidebands can be generated even in the case of normal dispersion.

Figure 2 shows the product $\delta\nu_m T_{\mathrm{FWHM}}$ as a function of the gain in the anomalous dispersion region for the first three sidebands by use of $\beta_2 = -5$ ps^2/km. For $\delta\nu_m T_{\mathrm{FWHM}} \lesssim 1$ the sidebands fall within the spectrum of the soliton, whereas for $\delta\nu_m T_{\mathrm{FWHM}} > 1$ the sidebands occur in the wings of the soliton spectrum. Figures 2(a) and 2(b) are drawn under identical operating conditions, except that $L = 100$ and 10 m, respectively. For both cavities the positions of the sidebands depend on the amplifier gain, which itself depends on the amount of cavity loss. Interestingly enough, the position of the first-order sideband peaks at a value close to 5 dB of gain but then moves inward as the gain increases and disappears altogether for an amplifier gain >13 dB. After that, the $m = 2$ curve essentially becomes the first sideband. Similar behavior occurs for the second- and higher-order sidebands. Many sidebands are likely to be observed for 100-m-or-longer

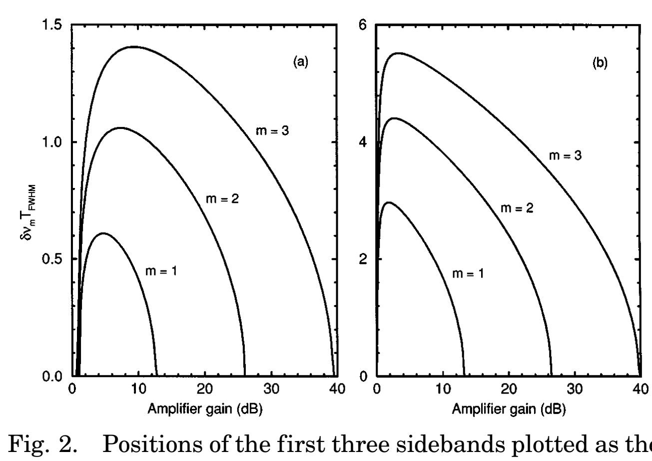

Fig. 2. Positions of the first three sidebands plotted as the product $\delta\nu_m T_{\mathrm{FWHM}}$ for the chirped soliton in the anomalous dispersion region as a function of the amplifier gain for cavity lengths of (a) 100 m and (b) 10 m.

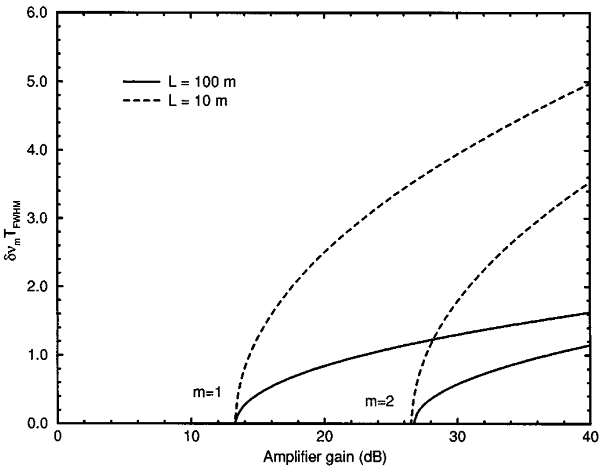

Fig. 3. Positions of the first two sidebands plotted as the product $\delta\nu_m T_{\mathrm{FWHM}}$ for a chirped soliton in the normal dispersion region as a function of the amplifier gain for cavity lengths of 100 and 10 m.

cavities, but only two or three sidebands may fall within the soliton spectrum.

For the shorter 10-m cavity the same qualitative curves for the side-mode positions are seen (Fig. 2b). The main difference is that the positions of the sidebands are much farther away from the center frequency of the soliton, as is also observed experimentally. These sidebands are expected to be weaker in amplitude since they are farther away from the peak of the gain curve.

Equation (9) also predicts sidebands in the normal dispersion regime, unlike in the case for the unchirped soliton. We show in Fig. 3 the product $\delta\nu_m T_{\mathrm{FWHM}}$ for the case of normal dispersion ($s = +1$) for the first two sidebands, using the same parameters as in Fig. 2. The sidebands for the 100- and 10-m cavities are indicated by the solid and the dashed curves, respectively. The main difference from the anomalous dispersion case is that only a few sidebands exist for normal dispersion for a given amplifier gain. Also, as the gain is increased, the next sideband that appears is actually closer to the center frequency of the soliton. Since sidebands have been seen in the spectra of pulses produced in neodymium-doped fibers[11] it is clear that soliton chirp plays an important role and must be included whenever sideband frequencies are compared experimentally and theoretically.

It should be noted that Eq. (9) applies to fiber lasers with cavities composed of fiber components that have similar dispersion characteristics. If there are large changes in dispersion in the cavity, as in the case of stretched-pulse mode-locked fiber lasers, the chirp of the pulse undergoes rapid changes in different fiber segments. In that case, since the propagation constant Γ of the chirped soliton changes with position in the cavity, the resonant coupling between the soliton and dispersive waves is likely to be suppressed.

In conclusion, we have shown that cavity losses are important in determining the positions of the soliton spectral sidebands. The imposed chirp on the soliton is directly affected by the amplifier gain, which depends on the cavity losses and shifts the positions of the sidebands as indicated by Eq. (9). At the same time, the sideband positions also depend on the net dispersion parameter $\beta_2 L$. Thus it seems possible to determine the chirps of the solitons produced by a fiber laser by measurement of the displacement of the sidebands from the soliton central frequency if the net dispersion parameter $\beta_2 L$ for the cavity is known accurately. By the same token, without consideration of the soliton chirp, measurements of sideband positions would be inadequate for determination of the dispersion of the laser cavity. To our knowledge, the effect of chirping in pulses emitted from fiber lasers on the soliton sideband spectra has not been studied experimentally.

L. W. Liou acknowledges support from the U.S. Department of Education for a graduate fellowship. The research is also supported in part by the U.S. Army Research Office.

References

1. J. P. Gordon, J. Opt. Soc. Am. B **9,** 91 (1992).
2. N. Pandit, D. U. Noske, S. M. J. Kelly, and J. R. Taylor, Electron. Lett. **28,** 455 (1992).
3. S. M. J. Kelly, Electron. Lett. **28,** 806 (1992).
4. D. U. Noske, N. Pandit, and J. R. Taylor, Opt. Lett. **17,** 1515 (1992).
5. N. J. Smith, K. J. Blow, and I. Andonovic, J. Lightwave Technol. **10,** 1329 (1992).
6. M. L. Dennis and I. N. Duling III, IEEE J. Quantum Electron. **30,** 1469 (1994).
7. H. A. Haus, E. P. Ippen, and K. Tamura, IEEE J. Quantum Electron. **30,** 200 (1994).
8. G. P. Agrawal, *Nonlinear Fiber Optics*, 2nd ed. (Academic, San Diego, Calif., 1995).
9. P. A. Bélanger, L. Gagnon, and C. Paré, Opt. Lett. **14,** 943 (1989).
10. G. P. Agrawal, Phys. Rev. E **48,** 2316 (1993).
11. M. Hofer, M. H. Ober, F. Haberl, and M. E. Fermann, IEEE J. Quantum Electron. **28,** 720 (1992).